

Structural evolution and kinetics in Cu-Zr metallic liquids from molecular dynamics simulationsLogan Ward,^{1,*} Dan Miracle,² Wolfgang Windl,¹ Oleg N. Senkov,² and Katharine Flores³¹*Department of Materials Science and Engineering, The Ohio State University, Columbus, Ohio 43210, USA*²*Materials and Manufacturing Directorate, Wright-Patterson Air Force Base, Ohio 45433, USA*³*Department of Mechanical Engineering and Materials Science, Washington University, St. Louis, Missouri 63130, USA*

(Received 14 May 2013; revised manuscript received 12 August 2013; published 23 October 2013)

The atomic structure of the supercooled liquid has often been discussed as a key source of glass formation in metals. The presence of icosahedrally coordinated clusters and their tendency to form networks have been identified as one possible structural trait leading to glass-forming ability in the Cu-Zr binary system. In this paper, we show that this theory is insufficient to explain glass formation at all compositions in that binary system. Instead, we propose that the formation of ideally packed clusters at the expense of atomic arrangements with excess or deficient free volume can explain glass forming by a similar mechanism. We show that this behavior is reflected in the structural relaxation of a metallic glass during constant pressure cooling and the time evolution of structure at a constant volume. We then demonstrate that this theory is sufficient to explain slowed diffusivity in compositions across the range of Cu-Zr metallic glasses.

DOI: [10.1103/PhysRevB.88.134205](https://doi.org/10.1103/PhysRevB.88.134205)

PACS number(s): 61.20.Ja, 61.20.Lc

I. INTRODUCTION

Especially in the past decade, there has been a large amount of discussion as to whether the structure of metallic liquid contributes to its ability to form a glass upon cooling. This idea dates back to a hypothesis by Frank that the stability of supercooled liquids can be explained by the prevalence of efficiently packed clusters that have symmetry incompatible with crystal formation and that icosahedrally coordinated clusters fill this role for single element systems.¹ More recent studies have considered how these efficiently packed clusters group together to form medium-range order in metallic glasses.^{2,3} Along with the energetic stability provided by these clusters, their effect on atomic mobility in the supercooled liquid has also been studied as a contributing reason for glass formation in metals.⁴

In particular, there has been a focus on the role of icosahedrally coordinated clusters as a basis for beneficial structural order. These clusters were found to be present in supercooled liquids of multicomponent alloys using x-ray diffraction.⁵ Via atomistic simulation, it was found that these clusters tend to form large, interconnecting networks in compositions known for forming bulk metallic glasses.⁶ That discovery has spurred a focus towards determining whether icosahedral clusters lead to slowed diffusion and, therefore, bulk metallic glass formation. In particular, it has been shown that the slowest atoms in a Cu-Zr liquid are generally associated with icosahedral clusters.⁴ It is also known that these clusters tend to agglomerate and form medium-range order,⁶ which has been found to further reduce atomic mobility in the liquid.⁷ Consequently, it is theorized that the formation of icosahedral short-range order and networks can contribute to glass formation in at least Cu-Zr-based alloys.

In this paper, we take a critical look at this structural component of glass-forming ability using the Cu-Zr binary as a trial system. We use molecular dynamics to show how structure changes with composition and attempt to draw trends with glass-forming ability. Additionally, we study the evolution of the amorphous structure with temperature during a constant-pressure quench from the liquid. We also perform a rapid quench from the liquid followed by evolution at a

constant volume and temperature to decouple the effects of temperature and density change from the effect of structural rearrangement. Our overall goal is to assess whether the present theories can be used to help explain glass-forming ability and structural rearrangements during cooling in this system. We then explore packing efficiency and “defective” clusters as a more generalized structural explanation.

II. METHODS

Copper-zirconium was chosen as a test system because metallic glasses are known to form between 25 to 72 at.% copper with several compositions that can be formed in fully amorphous castings over 1 mm in diameter, including alloys near Cu₆₄Zr₃₆, Cu₆₀Zr₄₀, Cu₅₆Zr₄₄, Cu₅₀Zr₅₀, Cu₄₆Zr₅₄, and Cu₄₅Zr₅₅.^{8–11} Many of the previous modeling studies discussed in Sec. I have been performed for this system,^{4,6,7} allowing direct comparison of our results. Additionally, interatomic potentials have been specifically developed to model liquid and glassy Cu-Zr, which allows for the use of classical molecular dynamics in this system.¹² For our purposes, using *ab initio* calculations would have severely limited the ability to study systems with large numbers of atoms on a long timescale.

A. Molecular dynamics

All simulations in this study were performed using large-scale atomic/molecular massively parallel simulator (LAMMPS).¹³ Bonding was described using Finnis-Sinclair-type many-body potentials developed by Mendelev *et al.* to model liquid and amorphous Cu-Zr.¹² Unless otherwise mentioned, temperature and pressure were controlled using a Nosé-Hoover thermostat,¹⁴ and an integration timestep of 2 fs was used.

B. Model generation

Models of metallic glasses were generated by starting with a bcc zirconium supercell containing 11 664 atoms that was randomly seeded with copper atoms to create compositions ranging from Cu₃₀Zr₇₀ to Cu₈₀Zr₂₀. This wide range was chosen to sample models on both sides of the isostructural

composition and, specifically, to include all compositions that are known to form bulk metallic glasses.⁸ Compositions were chosen (a) outside of the normal glass-forming range (Zr = 20, 30, 60, and 70 at.%), (b) at compositions known for high glass-forming ability (Zr = 35.7, 44, 50, and 54 at.%), and (c) compositions near those maxima (Zr = 38.2, 40, 46, 52, and 57 at.%).⁸

After initial relaxation, each model was heated under constant, zero pressure to 3000 K at 6.75×10^{13} K/s, held for 40 ps at that temperature and then quenched to 1500 K at 7.5×10^{11} K/s. At that point, the model was cooled in steps of 32.5 K at a nominal rate of 1.0×10^{11} K/s to 200 K. Starting at 1273 K, the time held at each temperature was increased by 12% from the previous step until 623 K. Below that temperature, the hold time at each step was decreased to the pre-1273 K length. This quench schedule was chosen to allocate extra simulation time to the supercooled liquid regime (which is between approximately 700 and 1000 K),⁸ where most of the structural arrangement occurs. Finally, each model was quenched to 0 K under constant pressure using a conjugate-gradient relaxation technique.

C. Structural analysis

The structure of each model was determined using a radical Voronoi tessellation.¹⁵ The atomic radii for copper and zirconium were taken to be the atomic radii of the pure metals, 1.26 and 1.58 Å.⁸ After using these radii to create a radical Voronoi tessellation model, faces smaller than 1% of the total surface area of each cell were removed in order to compensate for overcounting due to numerical issues inherent in the tessellation.¹⁶ The shape of the coordination polyhedron was determined by the shape of the Voronoi cell attributed to each atom and defined using the Voronoi index, $\langle n_3, n_4, n_5, n_6 \rangle$, where n_x is the number of atoms in the nearest-neighbor shell of the cluster that are connected to x other atoms in that shell.¹⁷ To characterize network formation, clusters are defined as connected if any atoms of the two clusters are nearest neighbors. This is consistent with medium-range order as described in a topological model for metallic glasses that views glass structure as an aggregation of independent clusters² but not with other atomistic studies where only clusters that share atoms are defined as connected.³ Once connections between clusters are determined, it is possible to locate distinct networks within the atomic structure.

D. Structural evolution at constant temperature

In order to partly decouple the effects of temperature and structural evolution during cooling, a rapid quench from the superheated liquid at 1500 K to the supercooled liquid at 800 K was performed at 3.5×10^{15} K/s under constant pressure and controlled temperature for cell compositions of $\text{Cu}_{64.3}\text{Zr}_{35.7}$ and $\text{Cu}_{50}\text{Zr}_{50}$. These compositions were chosen because they both are known for high glass-forming ability but have a large enough difference in composition that they should have different structures. The final hold temperature at 800 K is slightly above the glass transitions for both compositions, which were determined from the volume-temperature behavior during the quench simulation to be 765 and 710 K, respectively. Constant

volume was maintained during the structural evolution at the final hold temperature, and snapshots of the atomic positions were saved every 120 timesteps (480 fs).

E. Diffusivity calculation

During the simulations of structural evolution at constant temperature described in Sec. II D, parallel simulations were started every 60,000 timesteps (240 ps) in order to calculate the mean squared displacement rate of atoms at different points during the structural evolution. In these calculations, the structure evolved using the same ensemble (constant volume, constant temperature at 800 K), and snapshots of the atomic positions were saved every 3 ps for 150 ps. Diffusivity was calculated at several points during the hold by measuring the mean-squared displacement of atoms of each type and using the relationship

$$D = \lim_{t \rightarrow 150\text{ps}} \frac{1}{6} \frac{\delta}{\delta t} \langle |r(t + t_0) - r(t_0)|^2 \rangle. \quad (1)$$

F. Atomic packing efficiency

Atomic packing efficiency (APE) is a parameter used to approximate how much the packing efficiency of a cluster deviates from ideal.^{18,19} Unlike a direct calculation of volume packing efficiency, this parameter allows assessment of how close the system is to optimal packing, independent of cluster configuration and strain applied to the cluster. APE is defined as the radius ratio between the central atom and the average radius of atoms in the nearest-neighbor shell, normalized by the ideal radius ratio for a cluster with that number of atoms, which has been established in literature.²⁰ In this notation, the parameter is defined as

$$\text{APE} = \left(\frac{r_0}{r_1} \right) / R^*, \quad (2)$$

where r_0 is the radius of the central atom, r_1 is the mean radius of the nearest neighbors, and R^* is the optimal radius ratio of that cluster.^{8,18} An ideally packed cluster has an APE of 1, a cluster with excess free volume has an APE > 1, and one packed too closely has an APE < 1.

G. Cluster volume packing efficiency

The packing efficiency of a cluster is defined as the volume attributed to atoms inside a cluster divided by the total volume of the cluster and was calculated in a similar manner to previous work by Yang *et al.*²¹ The total volume can be determined by finding the volume of the convex polyhedron whose vertices are given by the centers of atoms in the nearest-neighbor shell. In order to determine the volume of the atoms inside the clusters, the convex hull polyhedron is first segmented into tetrahedra formed by the atoms at the corners of each face and the central atom. The solid angle of each atom inside each tetrahedron is then calculated using the relation provided by van Oosterom and Strackee.²² The fraction of the volume of an atom inside of the cluster is equivalent to its total solid angle included in all of the tetrahedra divided by 4π .

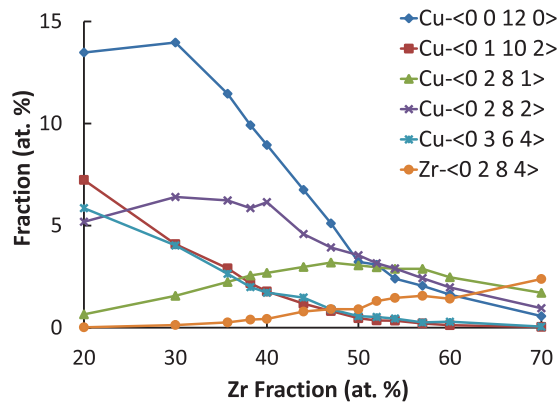


FIG. 1. (Color online) The most common atomic clusters identified in the amorphous structures of Cu-Zr metallic glasses with the Zr concentration ranging from 20 to 70 at.%. Each cluster is identified based on the species at the center and the polyhedron index (enclosed in angle brackets). The amorphous structures are the result of a quench from 1500 to 0 K at approximately 10^{11} K/s simulated using classical molecular dynamics.

III. RESULTS AND DISCUSSION

A. Composition dependence of icosahedral networks

The composition range chosen for our study samples structures with a wide distribution of short-range order, as shown by the fractions of the majority cluster types in Fig. 1. For example, in the composition range of 20 to 40 at.% Zr, there is a strong majority of Cu-centered full icosahedra ($\langle 0,0,12,0 \rangle$), while fewer than 3% of clusters have this topology in glasses with ≥ 50 at.% Zr. Taking only the fraction of a single-cluster type into account, there is no single cluster that can easily account for the glass-forming ability of copper-zirconium metallic glasses. Full icosahedra, which have been hypothesized to lead to improved glass-forming ability in metals, reach their maximum concentration near $\text{Cu}_{70}\text{Zr}_{30}$ —a composition that is not known to form bulk metallic glasses. Also, icosahedra are only present in small concentrations near the high zirconium fraction bulk metallic glass compositions, noted in previous work.²³ Even considering the other top clusters, no single-cluster topology shows a correlation with the compositions known for maximum glass-forming ability, which lie between $\text{Cu}_{64.3}\text{Zr}_{35.7}$ and $\text{Cu}_{46}\text{Zr}_{54}$.^{9–11} At most, the Cu-centered $\langle 0,2,8,1 \rangle$ clusters reach a broad, shallow maximum in this region, which alludes to but does not prove their importance in glass formation.

This raises the question of whether the coordination of several efficient clusters into a larger structure can explain local regions of improved glass-forming ability. A number of studies have shown that icosahedrally coordinated atoms tend to agglomerate into networks in some Cu-Zr-based metallic glasses.^{6,24} These structures have been hypothesized to be the source of slowed dynamics in metallic glasses, as atoms associated with icosahedra tend to change positions less frequently.⁴ While atomic mobility is even slower for agglomerated clusters,⁷ it has yet to be shown whether agglomerated clusters are unique to bulk metallic glasses or just an intrinsic property of supercooled liquids.

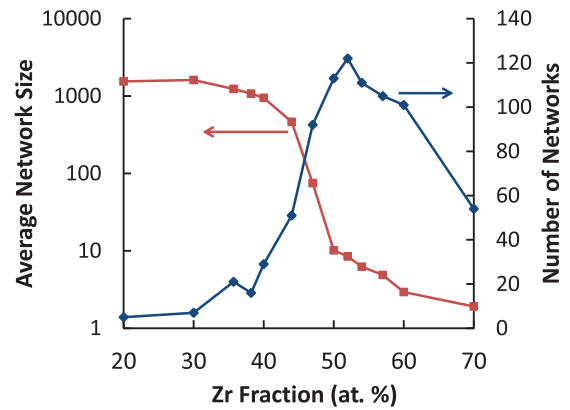


FIG. 2. (Color online) Average size and number of networks of icosahedrally coordinated atoms in Cu-Zr metallic glasses as a function of composition determined from the 0 K models of metallic glasses produced using molecular dynamics.

Figure 2 shows the number and average size of networks (i.e., number of clusters) of linked icosahedral clusters for several Cu-Zr compositions at 0 K. A large degree of interconnectivity is observed at low Zr concentrations; all of the icosahedra in systems with compositions less than approximately 40 at.% zirconium are connected by a much smaller number of large networks than in systems with higher Zr concentrations. This large degree of interconnectivity is unsurprising due to the large fraction of icosahedral clusters at low Zr concentrations, which is past the point (7.6 at.%), where it becomes impossible to pack icosahedra that do not share neighbors.

Based on current literature,^{7,24} these pervasive networks of icosahedra could be key features for glass formation in Cu-Zr metallic glasses. However, as found with the fraction of icosahedral clusters, the maximum network size occurs outside of the known glass-forming region, near $\text{Cu}_{70}\text{Zr}_{30}$. Also, the average network size decreases by two orders of magnitude between $\text{Cu}_{64.3}\text{Zr}_{35.7}$ and $\text{Cu}_{50}\text{Zr}_{50}$, yet both are known to have good glass-forming ability.⁸ Therefore, we conclude that this model is unable to explain glass-formation for all known glasses in this system and, more strongly, that the presence of these networks is neither a sufficient nor necessary condition for bulk metallic glass formation.

While pervasive networks of icosahedral clusters were found not to be unique to bulk metallic glass-forming liquids, there is still evidence to support that they play a role in bulk metallic glass formation. Several studies have attributed icosahedral clusters and their networks to locally stunted atomic mobility, but this leaves several questions open. Do these networks affect the *global* diffusivity? Why do these structures form?

B. Structural evolution during quenching

To help answer these questions, we investigated how the atomic structure of a Cu-Zr liquid changes during quenching. As shown in Fig. 3(a), the concentration of each of the most prevalent cluster types in a $\text{Cu}_{64.3}\text{Zr}_{35.7}$ glass increases during cooling. The total fraction of atoms with a coordination polyhedron matching one of these motifs changes from 6.8

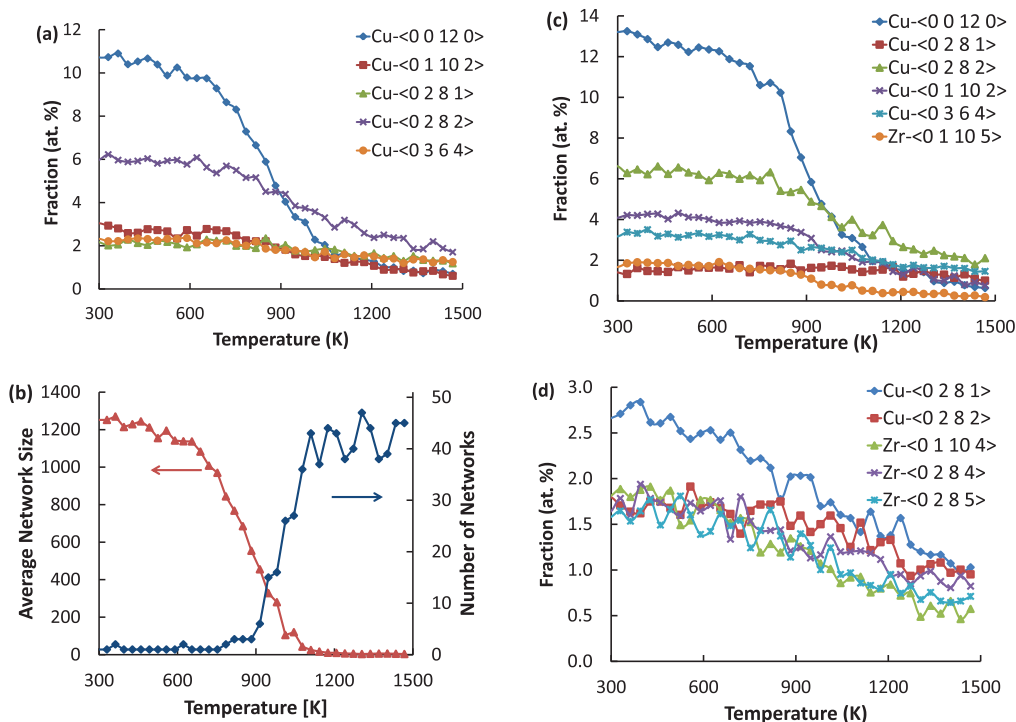


FIG. 3. (Color online) (a) The most prevalent clusters by Voronoi index and (b) average size and number of networks of icosahedral clusters in a $\text{Cu}_{64.3}\text{Zr}_{35.7}$ metallic glass as a function of temperature during a quench at 10^{11} K/s. The most prevalent clusters during cooling for (c) $\text{Cu}_{70}\text{Zr}_{30}$ and (d) $\text{Cu}_{30}\text{Zr}_{70}$ are also shown.

to 26.6% between 1500 and 300 K, suggesting that the structure becomes more homogenous at lower temperatures. In particular, the fraction of icosahedral clusters changes the most rapidly. Correspondingly, the size of networks formed by these clusters increases dramatically during cooling [see Fig. 3(b)].

A similar effect is visible in the evolution of polyhedron shapes during cooling in $\text{Cu}_{70}\text{Zr}_{30}$, as shown in Fig. 3(c). As with the other Cu-rich glasses, the total fraction of the most prevalent clusters increases during cooling. Also, the fraction of icosahedral clusters increases by around an order of magnitude during cooling, supporting the notion that this configuration is important in Cu-rich liquids. In the $\text{Cu}_{30}\text{Zr}_{70}$ model, the fraction of the most prominent clusters also grow in concentration during cooling as shown in Fig. 3(d). In general, our results suggest that regardless of which motifs are present, structural evolution during cooling can be characterized by homogenization of the liquid structure.

C. Constant temperature evolution

In order to decouple the effect of structural rearrangement from changes in temperature and sample density, we use a technique to study the development of structure at a constant temperature (described in Sec. IID). Before further testing the importance of network formation with this technique, we applied it to the model of a $\text{Cu}_{64.3}\text{Zr}_{35.7}$ glass in order to understand how well it replicated the features of a slower quench rate and thereby assess whether the structures are physically reasonable. As a result of the exceedingly high quench rate of over 10^{15} K/s before the constant temperature

holds, there is little structural change between the initial model at 1500 K and the model at 800 K after the quench. The partial coordination numbers of the Cu and Zr atoms do not change by more than 0.6%, which suggests little to no structural rearrangement took place.

The top four cluster types in the model also do not change before and after the quench, though their order does and their fractions change by 30%, on average. This fractional change is notable but is very small in comparison to the change in cluster fractions with temperature found at a slower quench rate [Fig. 3(a)], where, for example, the fraction of icosahedral clusters increases by approximately 790%. In comparison, this fraction only changes by 70% during the faster quench. After evolving the rapidly quenched model for 2 ns, the fractions of different cluster configurations (see Fig. 4) resemble the structure produced during the slower quench and stabilize after approximately 1 ns. Also, considering that the density of this liquid is within 2% of the slower-quenched structure, we conclude that the rapid quench freezes in the high-temperature liquid before the start of the hold and still results in a similar structure to a slower quench within accessible simulation times after holding at the lower temperature.

D. Network development

In order to study how networks of clusters form in metallic glasses, the structures of a $\text{Cu}_{64.3}\text{Zr}_{35.7}$ metallic glass generated during the simulated quench from 1500 to 200 K were studied. As shown in Fig. 3(b), the number of icosahedral networks remains near 40 between 1500 and 1050 K. In the temperature range 1050 to 800 K, the number of networks rapidly decreases

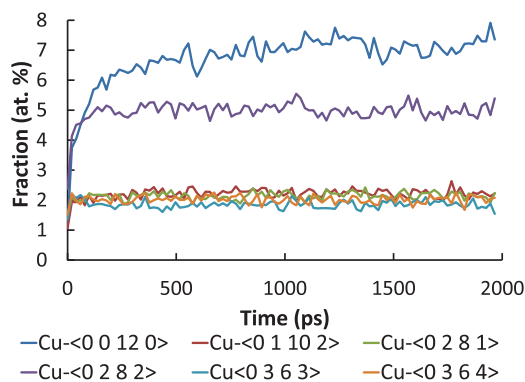


FIG. 4. (Color online) Fraction of top eight most prevalent Cu-centered clusters in $\text{Cu}_{64.3}\text{Zr}_{35.7}$ after a rapid quench from 1500 to 800 K as a function of time during a constant volume and temperature hold at 800 K.

to one, and at $T < 800$ K, only one network is identified. At the same time, the average size of the networks increases continuously with decreasing temperature. The trend is modest from 1500 K to ~ 1050 K, below which the size increases rapidly. This behavior suggests that the networks grow in size until they impinge to form a single network, which includes most of the atoms in the simulation. This hypothesis was tested by studying the constant temperature evolution of the same $\text{Cu}_{64.3}\text{Zr}_{35.7}$ model as described in Secs. II D and III C.

As mentioned in Sec. III C, the short-range order, viewed as the distribution of different cluster polyhedra topologies, rapidly changes during relaxation at 800 K. As shown in Fig. 4, the fraction of icosahedral clusters quickly increases from nearly nonexistent to the most prevalent structural feature in the first 230 ps, which makes the structure similar to that at 800 K for a slower quench rate [see Fig. 3(a)]. This fast rate of growth contributes to the quick formation of networks of icosahedral clusters, as shown in Fig. 5. The large number of small networks originally present at high temperature drops to fewer than five networks within ~ 500 ps of the relaxation time. By monitoring which atoms are present in the network, it was determined that the largest network at 500 ps continued to be the largest network at longer time periods and absorbed smaller networks, supporting the hypothesis of network coalescence.

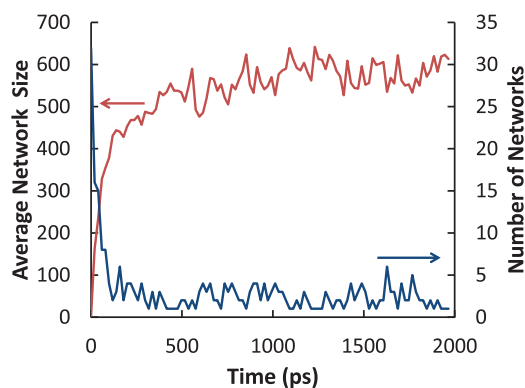


FIG. 5. (Color online) Evolution of networks of icosahedral clusters in a $\text{Cu}_{64.3}\text{Zr}_{35.7}$ metallic glass at 800 K after rapid quench from 1500 K.

This rapid formation of a single, pervasive network can be attributed to two factors: the large number of icosahedral clusters and the enhanced stability of agglomerated icosahedral clusters. Only 1.5 ns after the quench, around 50% of the atoms in the simulation are part of an icosahedral cluster. Additional clusters that form will likely be in close proximity or part of the network even without considering any bias to form as part of a network. Additionally, the network formation could be enhanced by the increased stability of networked icosahedral clusters, as demonstrated by Hao *et al.*⁷ Furthermore, within the time frame of 1500 to 2000 ps at 800 K, the average number of connected icosahedral clusters that remained stable, formed, or dissolved between snapshots of atomic positions 20 ps apart, was determined to be 13.03, 11.26, and 11.23, respectively. This provides evidence that stable icosahedral clusters are better connected, further suggesting the tendency of icosahedral clusters to aggregate into large networks.

E. Effect of structural relaxation at 800 K on the system energy and element diffusivity

Evolving the metallic glass structure at a constant temperature provides the unique ability to measure changes in system energy and global diffusivity because of structural change. Since the volume of the system is held constant, it is possible to decouple the effect of structural rearrangement from changes in free volume. As shown in Fig. 6(a), the total internal energy of the structure rapidly decreases during the first 100 ps and then continues decreasing but at a slower rate. This shows that the structure is relaxing into a lower energy state with the system volume held constant. The decrease in internal energy during evolution of the 1500-K structure at 800 K reinforces the idea that the structure in the liquid is strongly dependent on temperature and provides the additional observation that the most efficiently packed structure should not be viewed simply as the densest on a global scale.

Additionally, the diffusivity of the alloying elements in the liquid was studied as a function of time to assess whether the evolution in the structure can be attributed to stifled diffusion. As the diffusivity calculation in this study analyzes data from snapshots over an interval of 150 ps, it is not possible to make instantaneous measurements of diffusivity changes. Even so, it was possible to resolve that the diffusivity decreases by 60% within the first 250 ps of the simulation time [as shown in Fig. 6(b)], which is coincident with the growth of icosahedral short-range order and networks. Since icosahedral clusters locally reduce atomic mobility, and this behavior is enhanced for clusters present in networks,^{4,7} this observation supports the idea that the development of icosahedral order slows diffusivity.

To determine whether this is an effect of the icosahedral network formation, the same quench and hold experiment was performed with $\text{Cu}_{50}\text{Zr}_{50}$ —a composition with similar glass-forming ability to $\text{Cu}_{64.3}\text{Zr}_{35.7}$ but without the tendency to form large icosahedral networks. As shown in Figs. 7(a) and 7(b), the structural change in $\text{Cu}_{50}\text{Zr}_{50}$ is not as significant in terms of cluster topology or networks of icosahedral clusters in comparison to the copper-rich composition. Icosahedral clusters are not the most prevalent structural feature; and the network size only increases slightly after quenching. However,

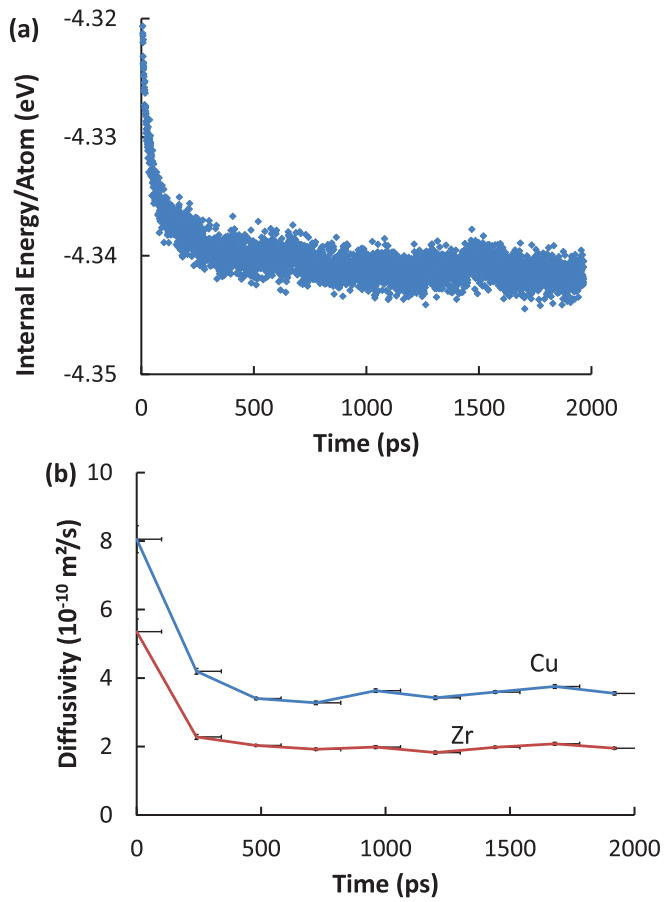


FIG. 6. (Color online) (a) Energy per atom and (b) diffusivity in $\text{Cu}_{64.3}\text{Zr}_{35.7}$ after a rapid quench from 1500 to 800 K as a function of time during a constant volume and temperature hold at 800 K. Error bars represent the time span used to calculate the diffusivity and the confidence interval from the diffusivity calculation.

there is still a change in the energy of the system over time and a drop in diffusivity after the quench [see Figs. 7(c) and 7(d)]. These small structural changes were found to correlate with a comparable change of 46% in diffusivity 200 ns after the rapid quench in comparison to 56% in $\text{Cu}_{64.3}\text{Zr}_{35.7}$. This change in diffusivity with only a minor change in icosahedral short-range order and networks does not disprove that networks of interconnected icosahedral clusters could contribute to slowing diffusion in supercooled liquids but shows they are not the only reason. In particular, the opinion that icosahedral clusters are the cause of stifled diffusivity lacks the ability to explain the change in diffusivity and energy of the clusters over time in $\text{Cu}_{50}\text{Zr}_{50}$.

F. Alternative explanation: Efficiently packed clusters and structural defects

Another way of conceptualizing this structural relaxation is to extend the view of structural defects developed by Egami *et al.*²⁵ This theory defines “defective” structural sites as atoms that experience either positive (tensile) or negative (compressive) local atomic stresses and corresponding volume strains. We extend this view here by noting that a defective structural site and its first shell of neighbors form an atomic cluster

whose packing efficiency is either higher (for compressive local stresses) or lower (for tensile local stresses) than ideal. We can thus track the presence of these defective sites using local packing efficiency and internal energy as proxies for volumetric strains.

The first parameter we use to investigate this concept in our models is the standard deviation of cluster volume packing efficiencies (see Sec. II G). Presumably, there is an ideal packing efficiency for each species in a metallic glass and, based on this theory, the average deviation from that ideal should decrease as the model becomes more relaxed. As shown in Fig. 8, the standard deviation of cluster packing efficiency decreases with temperature during quenching from 1500 to 300 K, which is consistent with the idea that defective sites are eliminated as the glass relaxes at lower temperatures. This concept of the elimination of “liquid-like” behavior on relaxation is also well supported by studies that examine other structural features of glasses, such as atom-level stresses.²⁶ Additionally, as shown in Fig. 9, the standard deviation of the packing efficiency of Cu-centered clusters rapidly decreases with time during the constant volume and temperature holds for both $\text{Cu}_{64.3}\text{Zr}_{35.7}$ and $\text{Cu}_{50}\text{Zr}_{50}$. This further provides evidence that we can attribute structural relaxation in the supercooled liquid to the elimination of defective clusters.

In order to further examine the idea that clusters with far-from-ideal packing efficiencies dissipate during relaxation, we used the APE parameter.¹⁸ As discussed in Sec. II F, this parameter describes the deviation of a cluster from the ideally packed one where any perfectly packed cluster has an APE of 1, clusters with excess free volume have an APE > 1, and those that are packed too tightly have an APE < 1. This allows us to determine whether a cluster is close to ideal packing irrespective of the magnitude of that cluster’s optimal packing efficiency. In effect, we can then determine if the system as a whole has reached a local maximum packing efficiency even if that consists of multiple cluster types, each with a unique optimal efficiency. This is especially important for amorphous materials, which are inherently structurally heterogeneous.

The mean and standard deviations of the APE of each cluster type both decrease as a function of temperature during a quench from 1500 to 300 K, as shown in Fig. 10. The mean decreases from approximately 1.022 to 1.005 during the quench, which implies that the average cluster loses free volume without becoming “over-packed.” The idea that a liquid loses free volume during cooling and still has some residual free volume is expected for an amorphous material. The deviation in APE also decreases, which implies a similar conclusion to what was developed based on the volume packing efficiency: elimination of clusters with far from ideal packing efficiencies is a key part of relaxation. Despite the remaining free volume after the relaxation, the magnitude of the standard deviation (~ 0.06) in combination with the average APE of 1.005 indicates that the final structure should not only have pockets of “free volume” (i.e., lower-density areas, APE > 1) but also higher-density areas (APE < 1).

The change in the APE of clusters was also studied during a constant volume and temperature simulation at 800 K in order to further explore its relationship with structural relaxation. During the first 200 ps of the hold, the mean APE for the $\text{Cu}_{64.3}\text{Zr}_{35.7}$ model dropped from 1.023 to

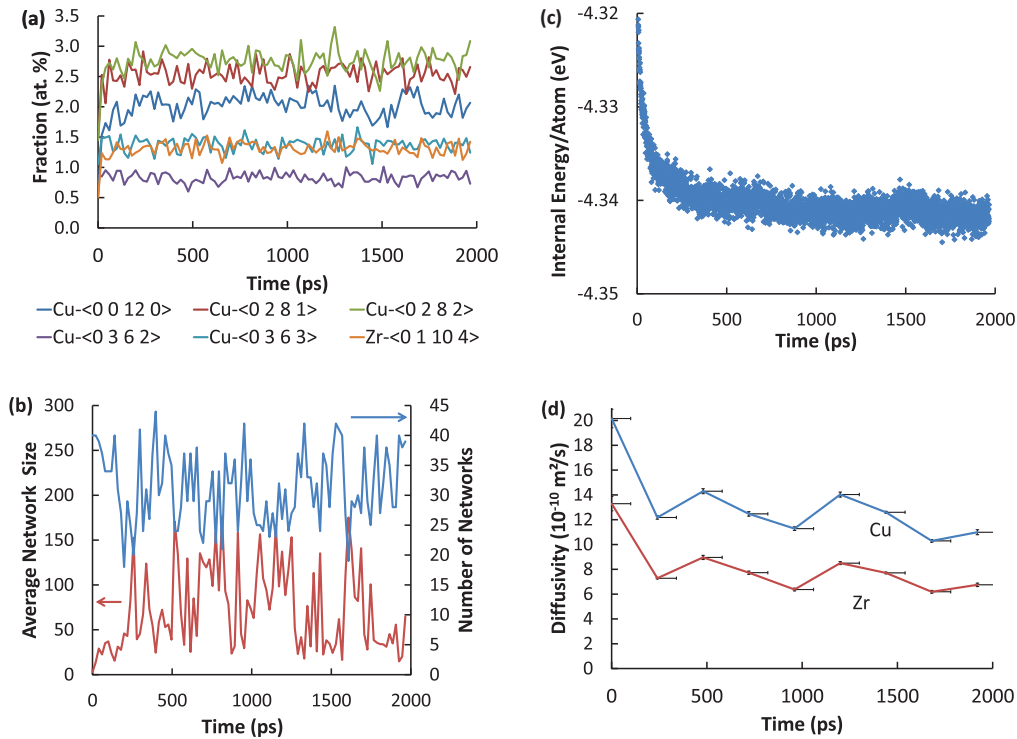


FIG. 7. (Color online) Changes in (a) five most prevalent cluster topologies and icosahedral clusters, (b) networks of icosahedral clusters, (c) energy per atom, and (d) diffusivity as a function of time for a Cu₅₀Zr₅₀ liquid after rapid quenching from 1500 to 800 K. Error bars represent the time span used to calculate the diffusivity and the confidence interval from the diffusivity calculation.

1.0098, which implies that the system adopted more efficiently packed local configurations. This change in packing efficiency with fixed volume is observable because the APE parameter only reflects the deviation of the packing from optimally efficient and does not change under the strain imposed by the constant volume condition since this measure does not explicitly take the positions of the atoms into account. The new atomic arrangements produced by the model are energetically favorable (as observed in the decrease in internal energy in Figs. 6 and 7) and, based on having an APE close to unity, would also be efficiently packed under conditions without the constant volume constraint. Additionally, the standard deviation reduces slightly from 0.080 to 0.063 over the first

200 ps. This shows that the system is rearranging into a new configuration that favors clusters with ideal packing by removing more defective ones. The same behavior is seen during the quench and hold simulation with Cu₅₀Zr₅₀, where the mean drops from 1.021 to 1.010 and the standard deviation drops from 8.38 to 6.99% during the first 200 ps. This shows that structural evolution by defect elimination takes place even in compositions with vastly different structural characteristics. Recall that the Cu_{64.3}Zr_{35.7} alloy has a large fraction of icosahedral clusters that form a network, which is not the case for the Cu₅₀Zr₅₀ alloy.

G. Comparison to existing theories

Recent work has shown that icosahedral clusters are not the most energetically stable clusters in metallic glasses.²⁷⁻³¹ Broadly consistent with this, this paper shows that the prevalence of icosahedral short-range order and networks does not give a compelling correlation with glass-forming composition regions. The formation of icosahedral clusters also cannot explain the decrease in diffusivity associated with the structural relaxation found in the Cu₅₀Zr₅₀ alloy. Taken together, these arguments suggest that there is no unique advantage in energetic stability or slowed dynamics specific to the formation of icosahedral order in metallic glasses.

The suggestion that the demise of the most defective clusters and the formation of more efficiently packed clusters gives structural relaxation and slowed diffusivity is consistent with the prevailing theory for why icosahedral clusters form and what that implies. However, the present work generalizes structure relaxation and slowed diffusivity in composition

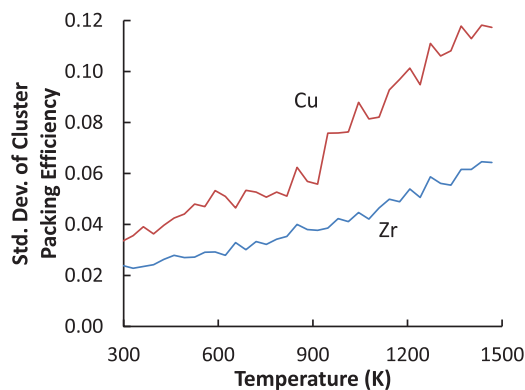


FIG. 8. (Color online) Standard deviation of cluster packing efficiency as a function of temperature in a Cu_{64.3}Zr_{35.7} metallic glass during a simulated quench from 1500 to 300 K at 10¹¹ K/s.

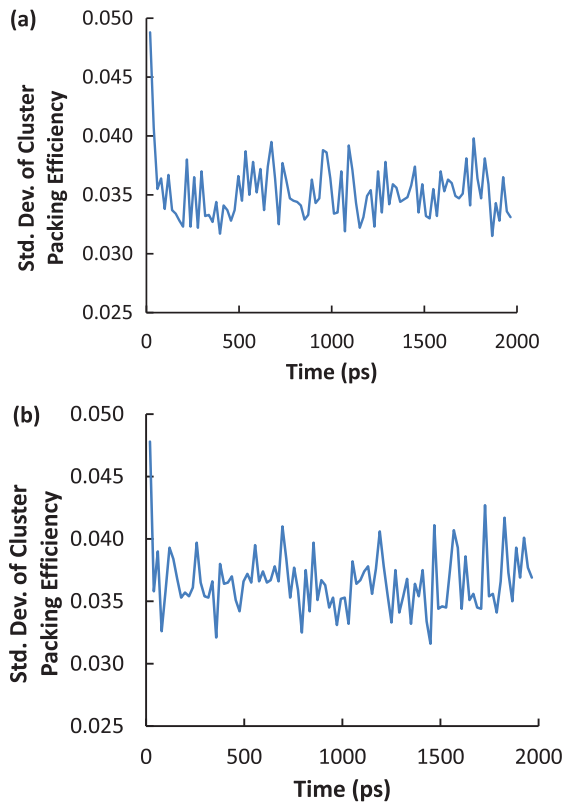


FIG. 9. (Color online) Standard deviation of the cluster packing efficiency of Cu-centered clusters for a (a) $\text{Cu}_{64.3}\text{Zr}_{35.7}$ and (b) $\text{Cu}_{50}\text{Zr}_{50}$ liquid during a constant volume and temperature hold at 800 K immediately following a rapid quench from 1500 K.

ranges, where icosahedral clusters are not favored to form. Thus, icosahedra do not exert a unique influence on glass-forming ability, and this effect is shared with other cluster types as well. The unifying feature, regardless of the topology, is the cluster packing efficiency and polytetrahedral-type short-range order of the prominent clusters.^{30,31} In this view, icosahedra play an important role in the stability of Cu-Zr glasses with ≤ 45 at.% Zr because they are the most efficiently packed cluster in this composition range. An icosahedrally coordinated cluster is efficiently packed when the ratio between the central atom's radius and the effective radius of the neighbors is approximately 0.902.²⁰ Copper-centered icosahedral clusters that contain approximately six to eight copper neighbors have the most nearly optimal packing efficiency, with radius ratios of 0.887, 0.904, and 0.922, respectively. These clusters have compositions between 30.8 and 46.2 at.% Zr, which is near the composition region, where the fraction of icosahedral clusters is the greatest. The maximum fraction of icosahedral clusters near this range could be attributed to a combination of driving forces of the system to minimize energy by increasing packing efficiency and the easy formation of clusters of these compositions given the system concentration. The high fraction of these clusters coupled with the enhanced stability of forming networks explains the formation of networks in that composition range.

The present analysis emphasizes the structural contribution to glass-forming ability. A complete understanding of glass-forming ability requires attention to structure, energetics,

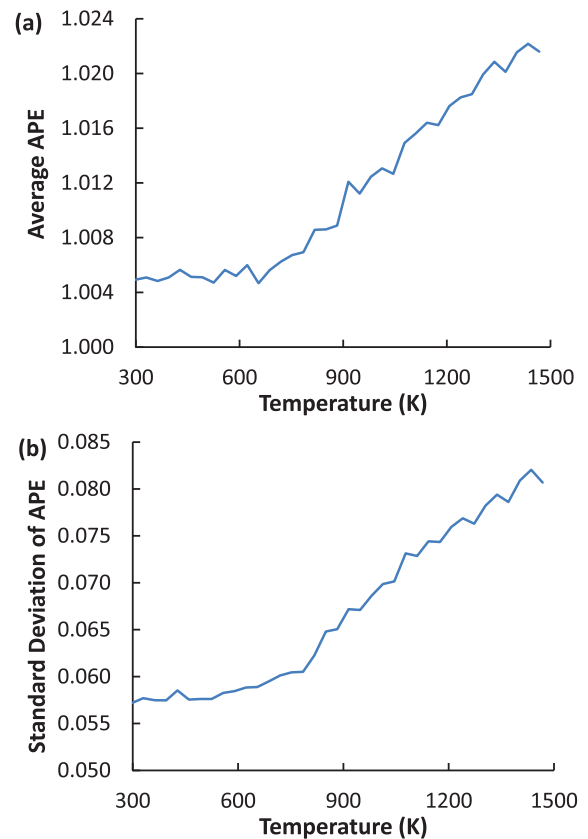


FIG. 10. (Color online) (a) Mean and (b) standard deviation of the APE of each cluster in a model of a $\text{Cu}_{64.3}\text{Zr}_{35.7}$ metallic glass during a quench from 1500 to 300 K at 10^{11} K/s.

and kinetics at a minimum. It is difficult to study these independently, and the present study shows that both energetics and kinetics are likely to depend on structure in subtle ways. While this paper does not give a final view, it does give a more generalized view of the structural contribution to glass stability, and some discussion of the connections between structure, internal energy, and kinetics.

H. Correlation between packing efficiency and cluster topology

Along with an alternative view of structural relaxation in metallic glasses, we also found that an alternative definition of cluster topology could be advantageous. Conventionally, the shape of an atom's coordination polyhedron is defined by the shape of the cell surrounding the atom in a Voronoi tessellation. Each face of this cell corresponds to a neighboring atom, which is classified as bonded to the central atom. The number of edges on a face of the cell indicates how many geometric connections that neighbor shares with other atoms bonded to the original atom. This information allows one to classify the shape of the atom's coordination polyhedron by counting the number of neighbors with a certain number of connections (see Sec. IIC).

While this method is effective in defining the shape of a coordination polyhedron, it ignores whether the neighboring atoms are actually bonded. Our proposal is that rather than considering neighboring atoms as connected if their associated faces share an edge, we only consider them connected if they

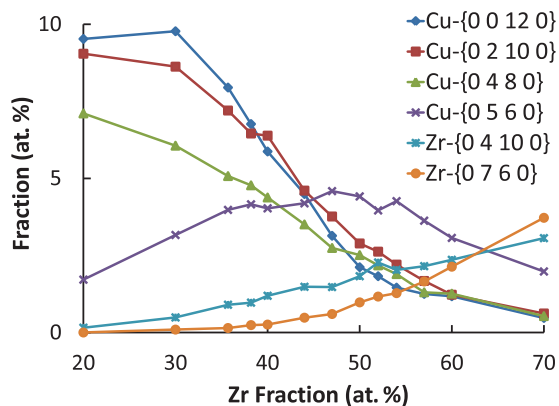


FIG. 11. (Color online) The most common cluster shapes as determined using a new definition for cluster topology in models of Cu-Zr metallic glasses generated using classical molecular dynamics.

are bonded (their own Voronoi cells share a face). This method should more accurately reflect the interactions between atoms in the first coordination shell, rather than simply reporting the geometry. Since it also defines shapes based on the connectivity (geometrical or otherwise), we can use the same index notation as before. For the purpose of this work, we will donate conventional coordination polyhedron shapes with angle brackets and those found using our new method with curly brackets.

Figure 11 shows the most prevalent clusters as determined using the new classification. There is still a majority of Cu atoms with 12 neighbors at Zr-lean compositions, a larger number of Cu atoms with 11 neighbors near $\text{Cu}_{50}\text{Zr}_{50}$, and many 14-coordinated Zr atoms at Zr-rich compositions (see Fig. 1 for comparison). However, the prevalent indexes are different. Instead of a simply a majority of icosahedral clusters (denoted as $\langle 0,0,12,0 \rangle$) in Zr-lean compositions, there are now also many icosahedral clusters missing a single bond between their neighbors ($\{0,2,10,0\}$). Rather than $\langle 0,2,8,2 \rangle$ being the most prevalent near $\text{Cu}_{50}\text{Zr}_{50}$, the index of the most prevalent cluster is now $\{0,5,6,0\}$ near $\text{Cu}_{50}\text{Zr}_{50}$. Therefore, the two methods give qualitatively similar results, although the actual cluster indexes are different.

The prevalence of certain cluster types, defined conventionally, is not as easy to explain based on their packing efficiency. While icosahedral and $\langle 0,2,8,2 \rangle$ clusters are both the most efficiently packed and prevalent near $\text{Cu}_{70}\text{Zr}_{30}$ [see Fig. 12(a)], this trend does not hold for glasses with higher Zr concentrations. Namely, the most efficiently packed and prevalent clusters do not correspond for any other alloy than $\text{Cu}_{30}\text{Zr}_{70}$.

In contrast, the cluster topologies defined using the alternative method can be explained much better. As shown in Fig. 12(b), icosahedral clusters (both $\{0,0,12,0\}$ and $\{0,2,10,0\}$) have the most ideal packing efficiency and, correspondingly, are the most prevalent. This fact suggests their importance and supports the hypothesis about their packing efficiency in Sec. III G. In the same way, the stability of Cu-Zr glasses with between 45 and 60 at.% Zr (including $\text{Cu}_{50}\text{Zr}_{50}$) will be strongly influenced by the most efficiently packed clusters in that compositional range. Copper-centered clusters with 11 neighboring atoms, $\{0,5,6,0\}$, are the best

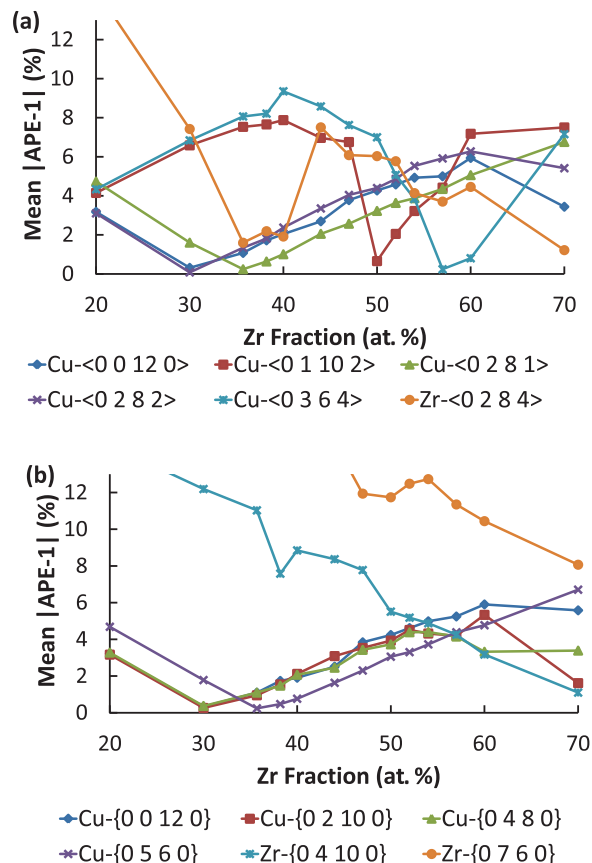


FIG. 12. (Color online) Mean deviation from ideal packing efficiency for the six most common cluster types defined (a) conventionally and (b) using our alternative method across composition region in Cu-Zr. Packing efficiency was measured using the APE parameter,¹⁸ where an APE of unity is ideally packed.

packed of the most common clusters in this composition range. Correspondingly, they were found to be the most prevalent structural feature in that set over most of the range (see Fig. 11). Additionally, as the liquid approaches a composition of 70 at.% Zr, Zr-centered clusters with 13 neighbors ($\{0,7,6,0\}$) are the most efficiently packed and most prevalent.

This agreement suggests that the structure of metallic liquids may be better described using our alternative method for defining the coordination polyhedra. Additionally, it demonstrates that the theory described in this work provides a framework for understanding what structures tend to form in metallic glasses, which could allow for an improved understanding of how structure influences glass-forming ability in metals.

IV. CONCLUSION

In this paper, we studied the evolution of structure and properties of a Cu-Zr metallic liquid during cooling and evolution at constant volume and temperature. It was found that the development of icosahedral order fails to explain the observed diffusivity and energy changes in $\text{Cu}_{50}\text{Zr}_{50}$. This paper develops a more general view that ideally packed atomic clusters are formed at the expense of clusters with excess or deficient free-volume during structural relaxation of a metallic glass, which supports earlier work by Egami

*et al.*²⁵ The proposed model also explains slowed diffusivity in compositions and alloy systems that do not show a propensity for forming icosahedrally coordinated clusters and provides a framework for understanding why the formation of networks of icosahedral clusters is correlated with slowed dynamics.

ACKNOWLEDGMENTS

The work at Ohio State and Washington University was funded by the Defense Threat Reduction Agency under Grant No. HDTRA1-11-0047 and by the Air Force Office

of Scientific Research under Grant No. FA9550-09-1-0251. Simulations were performed at the Ohio Supercomputer Center (Grant No. PAS0072). L.W. was supported by the Department of Defense through the National Defense Science and Engineering Graduate Fellowship Program and the Ryan Fellowship at Northwestern University.

The work at the Air Force Research Laboratory was supported through the Air Force Office of Scientific Research (M. Berman, Program Manager, Grant No. 10RX14COR) and the Air Force under onsite Contract No. FA8650-10-D-5226 conducted through UES, Inc., Dayton, Ohio.

*Present address: Department of Materials Science and Engineering, Northwestern University, Evanston, Illinois 60208, USA.

¹F. C. Frank, *Proc. R. Soc. London, Sect. A* **215**, 43 (1952).

²D. B. Miracle, *Nat. Mater.* **3**, 697 (2004).

³H. W. Sheng, W. K. Luo, F. M. Alamgir, J. M. Bai, and E. Ma, *Nature (London)* **439**, 419 (2006).

⁴Y. Q. Cheng, H. W. Sheng, and E. Ma, *Phys. Rev. B* **78**, 014207 (2008).

⁵G. W. Lee, A. Gangopadhyay, T. K. Croat, T. J. Rathz, R. W. Hyers, J. R. Rogers, and K. F. Kelton, *Phys. Rev. B* **72**, 174107 (2005).

⁶Y. Q. Cheng, E. Ma, and H. W. Sheng, *Phys. Rev. Lett.* **102**, 245501 (2009).

⁷S. G. Hao, C. Z. Wang, M. Z. Li, R. Napolitano, and K. M. Ho, *Phys. Rev. B* **84**, 064203 (2011).

⁸D. B. Miracle, D. V. Louzguine-Luzgin, L. V. Louzguina-Luzgina, and A. Inoue, *Int. Mater. Rev.* **55**, 218 (2010).

⁹D. Xu, B. Lohwongwatana, G. Duan, W. L. Johnson, and C. Garland, *Acta Mater.* **52**, 2621 (2004).

¹⁰P. Yu and H. Bai, *J. Mater. Res.* **21**, 1674 (2006).

¹¹D. Xu, Ph.D. thesis, California Institute of Technology, 2005.

¹²M. I. Mendeleev, M. J. Kramer, R. T. Ott, D. J. Sordelet, D. Yagodin, and P. Popel, *Philos. Mag.* **89**, 967 (2009).

¹³S. Plimpton, *J. Comput. Phys.* **117**, 1 (1995).

¹⁴W. Hoover, *Phys. Rev. A* **31**, 1695 (1985).

¹⁵B. Gellatly, *J. Non-Cryst. Solids* **50**, 313 (1982).

¹⁶W. Brostow, M. Chybicki, R. Laskowski, and J. Rybicki, *Phys. Rev. B* **57**, 13448 (1998).

¹⁷J. L. Finney, *Proc. R. Soc. London, Sect. A* **319**, 479 (1970).

¹⁸K. J. Laws, K. F. Shamlaye, K. Wong, B. Gun, and M. Ferry, *Metall. Mater. Trans. A* **41**, 1699 (2010).

¹⁹Q. Wang, J. B. Qiang, J. H. Xia, J. Wu, Y. M. Wang, and C. Dong, *Intermetallics* **15**, 711 (2007).

²⁰D. B. Miracle, E. A. Lord, and S. Ranganathan, *Mater. Trans.* **47**, 1737 (2006).

²¹L. Yang, G. Guo, L. Y. Chen, C. L. Huang, T. Ge, D. Chen, P. K. Liaw, K. Saksl, Y. Ren, Q. S. Zeng, B. LaQua, F. G. Chen, and J. Z. Jiang, *Phys. Rev. Lett.* **109**, 105502 (2012).

²²A. Van Oosterom and J. Strackee, *IEEE Trans. Biomed. Eng. BME-* **30**, 125 (1983).

²³Y. Q. Cheng, A. J. Cao, H. W. Sheng, and E. Ma, *Acta Mater.* **56**, 5263 (2008).

²⁴M. Z. Li, C. Z. Wang, S. Hao, M. J. Kramer, and K. M. Ho, *Phys. Rev. B* **80**, 184201 (2009).

²⁵T. Egami, V. A. Levashov, J. R. Morris, and O. Haruyama, *Metall. Mater. Trans. A* **41**, 1628 (2010).

²⁶Y. Q. Cheng, E. Ma, *Prog. Mater. Sci.* **56**, 379 (2011).

²⁷S. G. Hao, C. Z. Wang, M. J. Kramer, and K. M. Ho, *J. Appl. Phys.* **107**, 053511 (2010).

²⁸Q. K. Li and M. Li, *Chin. Sci. Bull.* **56**, 3897 (2011).

²⁹O. N. Senkov, D. B. Miracle, E. R. Barney, A. C. Hannon, Y. Q. Cheng, E. Ma, *Phys. Rev. B* **82**, 104206 (2010).

³⁰O. N. Senkov, Y. Q. Cheng, D. B. Miracle, R. Barney, A. C. Hannon, and C. F. Woodward, *J. Appl. Phys.* **111**, 123515 (2012).

³¹O. N. Senkov and Y. Q. Cheng, *Metall. Mater. Trans. A* **44**, 1980 (2013).